

ENTRAINMENT OF COAL PARTICLES IN A GAS FLUIDIZED BED

Yong Seung YOON, Sang Done KIM* and Won Hoon PARK**

Department of Chemical Engineering, Korea Advanced Institute of Science and Technology
Seoul, 131 Korea

**Korea Institute of Energy and Resources Daejeon, Korea

(Received 7 March 1986 • accepted 31 July 1986)

Abstract—Entrainment from an air fluidized bed of coal particles in a 14.5 cm-ID column has been studied. The effects of gas velocity and mean particle size on the transport disengaging height(TDH) and entrainment rate have been determined. The entrainment rate increased with the increase in the fluidizing air velocity but decreased with increase in the mean particle size and the column height above the fluidized bed. The date of entrainment rate and the TDH have been correlated in terms of Froude and Archimedes numbers.

INTRODUCTION

The entrainment of solids above a fluidized bed is a prime disadvantage of fluid bed operation since the loss of fines due to the entrainment resulted in catalyst cost, pollution abatement problem and loss of reaction rates, etc. Recently, coal combustion in a fluidized bed combustor has been a subject of worldwide interest. The low grade coals can be utilized for industrial and utility power generation whereas the higher grade coals shall preferentially used for petroleum feedstocks, synthetic fuels and metallurgical processes. In a fluidized bed combustor, one of the main cause for the decrease in the combustion efficiency is known to be the entrainment of coal fines from the combustor [1, 2]. Therefore, the knowledge of the entrainment pattern above the bed and transport disengaging height(TDH) is indispensable for an efficient design of coal combustors, cyclones, and coal gasifiers, etc.

Therefore, in the present study, the effects of air velocity (0.3-1.4 m/s), and coal particle size (0.12-0.5 mm) on the entrainment rate and the TDH have been determined.

EXPERIMENTAL

Experiments were carried out at room temperature and atmospheric pressure in a 14.5 cm-ID × 240 cm

high plexiglas column which is shown in schematically in Fig. 1. The main section of the column was constructed from three pieces of 14.5 cm-ID × 80 cm-high × 0.6 cm-thick plexiglas cylinder flanged together.

The solid particles were supported on a perforated plate which served as the gas distributor (Table 1).

The oil free compressor air through a pressure regulator, a filter and calibrated rotameters was fed to the wind box in which a perforated plate was placed for even air distribution.

Pressure taps were mounted flush with the column wall at 10 cm height intervals. The static pressure at each of these points was measured with a 45 degree declined liquid paraffin manometer. From this measurement, pressure profiles along the bed height were obtained to determine the expanded bed height and the bed density.

The entrained solid particles were sucked through a suction probe which was made of glass tube. The diameter of the probe mouth was 1.0 cm and its diameter was reduced to 0.6 cm in order to accelerate the collected solids into the suction chamber to prevent saltation in the transfer line. The particle loaded air entered a paper filter thimble where all the fines were trapped. The thimbles were enclosed in a large chamber from which clean air was sucked by a vacuum pump. The flow rate of air was measured with a rotameter and the pressure in the chamber was measured by a vacuum gauge. The position of the probe tip was located by means of a graduated scale.

The initial solid bed height was maintained at 30 cm.

* to whom all correspondence should be addressed.

**present address: Division of Chemical Engineering, KAIST, Seoul, Korea.

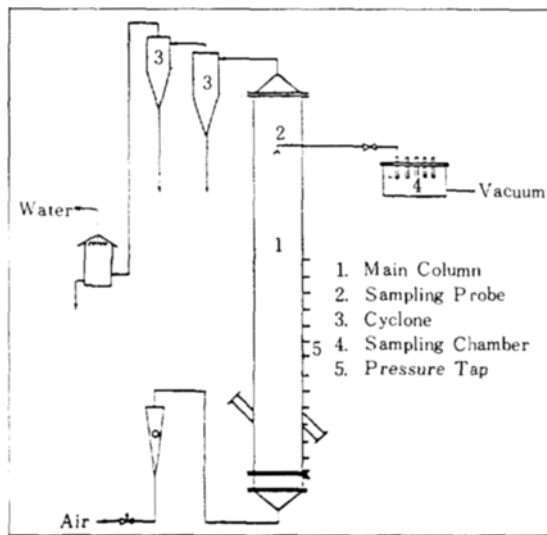


Fig. 1. Experimental apparatus.

The bed of solids were fluidized by air whose velocity ranged from 30.5 to 137.2 cm/s depending on the particle size.

Ten sampling ports were located at 57, 74, 94, 114, 134, 159, 174, 194, 214 and 234 cm from the distributor plate. In order to obtain an accurate solid sample, the suction flow rate of air through the probe mouth was maintained at the average superficial velocity in the column. At the given air velocity, point samples were taken for 3 min. across the radius of the column at a number of heights above the bed.

The entrainment rate constant was determined from the knowledge of the weight of solids, dW , collected at the given sampling time, dt , in a given cross sectional area of the column, A , as

$$E = dW/A \cdot dt \quad (1)$$

Table 1. Summary of the experimental conditions.

Material	Coal Ash:33.9% Moisture:6.32% Fixed carbon:55.14% Volatile Matter:4.64%
Particle diameter (mesh)	-28+40, -40+60, -60+100, -100+140
Particle density	2.0 g/cm ³
Initial bed height	0.3 m
Air velocity range	0.3 ~ 1.37 m/s
Distributor (perforated plate)	opening area, %:1.05 hole size:1.0 mm

The expanded bed height was determined from the plot of the static pressure against column height where the expanded bed height was taken as the point at which a change in the slope of the plot was observed.

The details of coal samples and the operating variables are summarized in Table 1.

RESULTS AND DISCUSSION

TDH is defined as the height above the bed at which the entrainment rate and particle size distribution become essentially constant [3]. Therefore, TDH can be determined from the difference between the height of the equilibrium stage and the expanded bed height. The expanded bed height increased with increase in air velocity.

The entrainment rate along the column height is shown in Fig. 2. As can be seen in the figure, the change of entrainment rate has two distinct stages [3], namely, the kinetic stage in which the rate decreases with the bed height and the equilibrium stage in which the rate is independent of the bed height. From the figure, the equilibrium stage height was taken as the point at which a change in the slope of the plot was observed. In the kinetic stage, the particles are entrained by the kinetic force from the bubble breakage at the given bed surface. Thus, the entrainment rate decreases with the column

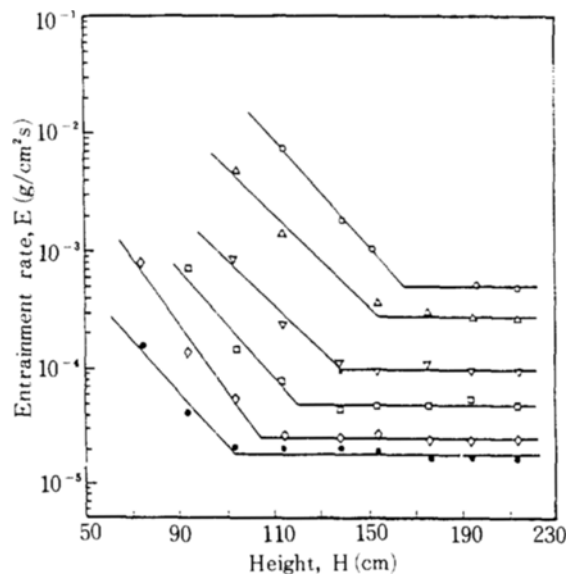


Fig. 2. Entrainment rate along the column height ($d_p = 0.333$ mm).

U_g (cm/s):

○ 137.2 △ 121.9 ▽ 106.7 □ 91.4 ◇ 76.2 ● 61.0

height. The amount of kinetic energy may depend more on the frequency of bubble breakage than on the bubble size [4].

The entrained rate decreases exponentially with the bed height (Fig. 2) in the kinetic stage [5]. Thereby, the TDH is equivalent to the height of the equilibrium stage.

Effect of Gas Velocity on the Entrainment Rate

The entrainment of the fines from a fluidized bed consisting of a wide size spectrum will occur when the gas velocity exceeds the particle terminal velocity. The gas bubbles carry the fines and throw the fines up above the bed surface with an eruption of bubbles since the actual local gas velocity is much higher than the superficial velocity in the bed. Therefore, above the TDH, the entrainment rate increased exponentially with gas velocity (Fig. 3). For the sake of comparison, the data of previous studies [6,7] are also plotted in the figure. As can be seen in the figure, the entrainment rate is proportional to the 3rd. to 6th. power of the air velocity. This is consistent with the data of the previous studies [6,7]. However, the entrainment rate slightly decreased with the column height above the height of equilibrium stage at the lower gas velocity [8,9] due to the small inertia force.

The values of entrainment rate collected in the present study are lower than the values from the correlation of Zenz and Weil [7]. This may be due to the differences in the particle size (11-168 μm), the solid properties (FCC), and the range of air velocity employed (31-72

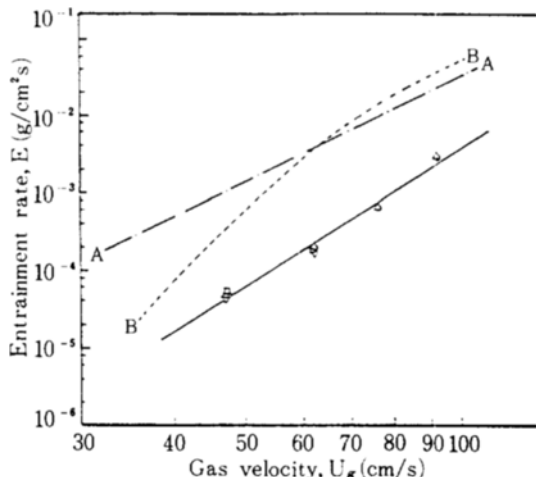


Fig. 3. Effect of gas velocity on entrainment rate at the height above TDH($dp = 0.198 \text{ mm}$).

∇ \circ \square \triangle
 $H(\text{cm})$: 234 214 194 174
A: Correlation of Zenz and Weil(7)
B: Correlation of Merrick and Highley(6)

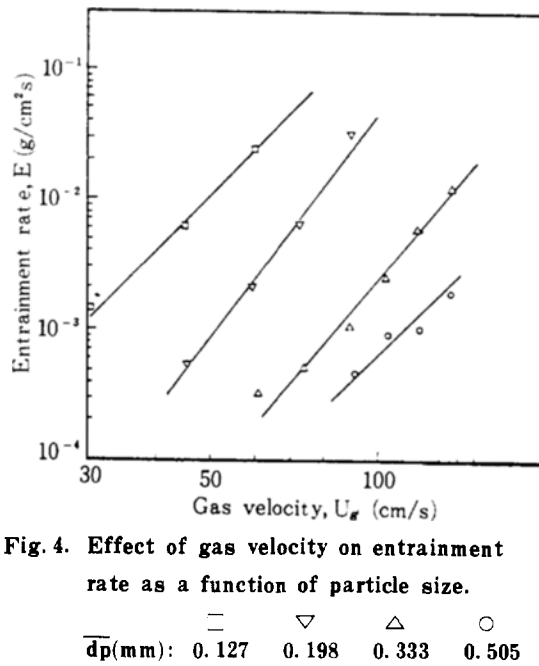


Fig. 4. Effect of gas velocity on entrainment rate as a function of particle size.

\square ∇ \triangle \circ
 $\overline{dp}(\text{mm})$: 0.127 0.198 0.333 0.505

cm/s). In addition, the data from the correlation of Merrick and Highley [6] exhibit higher or lower values of entrainment rates in the beds of different particle sizes since their data were obtained from a fluidized bed combustion pilot plant using the wide particle size distribution (0-2000 μm). Also, their empirical correlation for the elutriation rate was below the TDH.

Effect of Mean Particle Size on the Entrainment Rate

The variation of entrainment rate due to the mean particle size can be seen in Fig. 4 as a function of air velocity. As can be expected, the entrainment rate increased with the decrease in the mean particle size at a given air velocity since the particle terminal velocity is proportional to particle diameter.

The mean particle size of the entrained solids is plotted against the inverse Froude number in Fig. 5. As can be seen in the figure, there are three regions. The mean particle size drop-off rapidly at the value of the inverse Froude number in which the momentum of the bursting bubbles is of importance. However, the rate of drop-off gradually decreased as the inverse Froude number increased. However, the dependence of the mean particle size on the inverse Froude number gradually diminished and it levelled off at about the inverse Froude number of 30 [9]. This value is far smaller than that in the bed of fresh cracking catalyst ($dp = 58 \mu\text{m}$) fluidized by air in 61 cm-ID column [9]. This difference may be due to the differences of particle (FCC) properties (size and density) and the geometry of fluidized bed em-

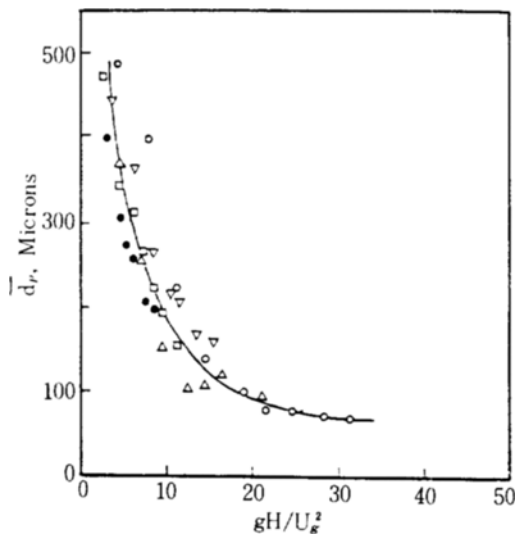


Fig. 5. Plot of the geometric mean diameter of the entrained particle against inverse Froude number.

○ △ ▽ □ ●
 U_g (cm/s): 76.2 91.5 106.7 121.9 137.2

ployed.

Radial Entrainment Profiles

A typical radial profile of the velocity obtained in the column is shown in Fig. 6. In general, such profiles were always relatively flat and exhibited the shape characteristics of turbulent flow profiles. It may indicate that the entrained particles in the bed was sucked by air through the sampling probe at the average superficial velocity.

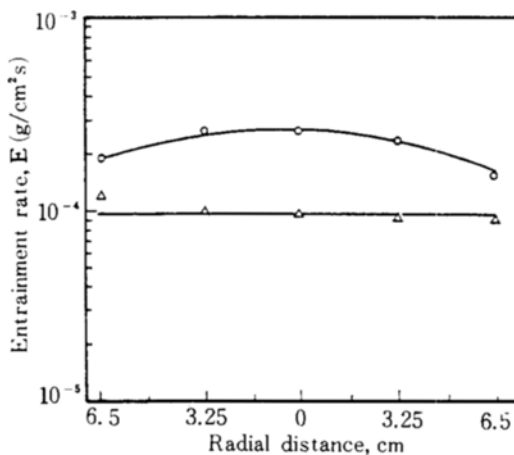


Fig. 6. Radial profile of entrainment rate.
 $(d_p = 0.198 \text{ mm}, U_g = 45.7 \text{ cm/s})$
 Height from the Distributor(cm): △; 214
 ○; 114

Also, the radial profiles become flatter with the increase in the column height [10]. This radial profile coincides with the data of the previous studies [9, 10, 11]. The downward flow of dense clusters along the column wall was observed below the equilibrium stage height and the concentration of solids in the vicinity of the wall may be much higher than that in the center of the column [11]. However, above the equilibrium stage height, the downward flow of solid particles is negligibly small so that the entrainment rate which was measured at the center of the column can be represented as a mean value across the column radius.

Correlation of Entrainment Rate and TDH

The entrainment in terms of the ratio of mass flux of solids to mass flux of gas in the present and previous studies [5, 7, 8, 10-14] have been correlated in terms of Froude and Archimedes numbers as

$$\frac{\rho_s U_s}{E} = 1.86 \times 10^6 \text{ Ar}^{0.18} \text{ Fr}^{-2.50} \quad (2)$$

where the correlation coefficient is 0.88. This correlation covers the range of variables $2.45 < \text{Ar} < 43200$ and $40 < \text{Fr} < 6468$.

Also, the data of TDH of the present and of previous studies [7, 8] have been correlated with the above dimensionless terms as

$$\frac{\text{TDH}}{D_c} = 1.38 \text{ Ar}^{0.42} \text{ Fr}^{-0.07} \quad (3)$$

where the correlation coefficient is 0.92. Eq. (3) covers the range of variables $17.2 < \text{Ar} < 8803$ and $2.48 < \text{Fr} < 973$.

In summary, the entrainment rate decreased with the column height above the TDH and the mean particle size but it increased with the air velocity. The transport disengaging height (TDH) of coal particles was found to be higher than the other particles such as sand or glass beads and it decreased with the mean particle size.

The values of the entrainment rate and TDH have been correlated in terms of Froude and Archimedes numbers.

NOMENCLATURE

- A : cross sectional area of column, cm^2
- Ar : Archimedes number, $d_p^3 \rho_s (\rho_p - \rho_s) g / \mu^2$
- Dc : column diameter, cm
- dp : particle diameter, cm
- E : entrainment rate, $\text{g/cm}^2 \cdot \text{s}$
- Fr : Froude number, U_g^2 / gH
- g : acceleration due to gravity, cm/s^2
- H : column height, cm
- TDH : transport disengaging height, cm
- Ug : gas velocity, cm/s
- W : weight of solids, g

Greek Letters

ρ_g : gas density, g/cm³
 ρ_p : particle density, g/cm³
 μ : fluid viscosity, mPa s

REFERENCES

1. Bak, Y.C., Son, J.E. and Kim, S.D.: *Hwahak Konghak*, **23**, 4 (1985).
2. Choi, J.C., Kim, Y.J., Moon, S.H. and Kim, S.D.: *Hwahak Konghak*, **23**, 153 (1985).
3. Sycheva, T.N. and Donat, E.V.: *Int. Chem. Eng.*, **10**, 172 (1970).
4. Zenz, F.A.: *Hydrocarbon Processing*, 110 (1974).
5. Andrews, J.M.: *Ind. Eng. Chem.*, **52**, 85 (1960).
6. Merrick, D. and Highley, J.: *AIChE Symp. Ser.*, **70**, 366 (1972).
7. Zenz, F.A. and Weil, N.A.: *AIChE J.*, **4**, 472 (1958).
8. Amitin, A.V., Martyushin, I.G. and Gurevich, D.A.: *Chem. and Tech. of Fuels and Oil*, **3**, 181 (1968).
9. Fournol, A.B., Bergougou, M.A. and Baker, C.G.J.: *Can. J. Chem. Eng.*, **51**, 401 (1973).
10. Geldart, D., Cullinan, J., Georghiades, S., Gilvray, D. and Pope, D.J.: *Trans. Inst. Chem. Eng.*, **57**, 269 (1979).
11. George, S.E. and Grace, J.R.: *AIChE Symp. Ser.*, **74**, 67 (1978).
12. Large, J.F., Matinie, Y. and Bergougou, M.A.: *Intl. Powder Bulk Solids Handling & Processing Conf.*, Chicago (1976).
13. Lewis, W.K., Gilliland, E.R. and Lang, P.M.: *Chem. Eng. Progr. Symp. Ser.*, **38**, 65 (1962).
14. Morooka, S., Kawazuishi, K. and Kato, Y.: *Powder Technol.*, **26**, 75 (1980).